

# Journal of Materials Chemistry B

Accepted Manuscript



This article can be cited before page numbers have been issued, to do this please use: X. Song, N. Li, C. Wang and Y. Xiao, *J. Mater. Chem. B*, 2016, DOI: 10.1039/C6TB02524B.



This is an Accepted Manuscript, which has been through the Royal Society of Chemistry peer review process and has been accepted for publication.

Accepted Manuscripts are published online shortly after acceptance, before technical editing, formatting and proof reading. Using this free service, authors can make their results available to the community, in citable form, before we publish the edited article. We will replace this Accepted Manuscript with the edited and formatted Advance Article as soon as it is available.

You can find more information about Accepted Manuscripts in the [author guidelines](#).

Please note that technical editing may introduce minor changes to the text and/or graphics, which may alter content. The journal's standard [Terms & Conditions](#) and the ethical guidelines, outlined in our [author and reviewer resource centre](#), still apply. In no event shall the Royal Society of Chemistry be held responsible for any errors or omissions in this Accepted Manuscript or any consequences arising from the use of any information it contains.



Journal Name

ARTICLE

## Targetable and Fixable Rotor for Quantifying Mitochondrial Viscosity of Living Cells by Fluorescence Lifetime Imaging

Xinbo Song,<sup>a</sup> Ning Li,<sup>a</sup> Chao Wang,<sup>a</sup> and Yi Xiao<sup>a\*</sup>Received 00th January 20xx,  
Accepted 00th January 20xx

DOI: 10.1039/x0xx00000x

www.rsc.org/

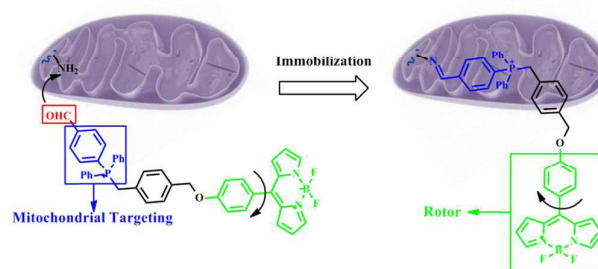
It is meaningful to accurately quantify the changes of local viscosity within mitochondria of living cells, because viscosity influences the mitochondrial network organization and the metabolite diffusion. Although many molecular probes targeting mitochondria have been reported, almost all of them are not fixed to the mitochondria. Thus, they may not be suitable for sensing in abnormal mitochondria with lowered potential. In order to monitor viscosity in all mitochondria, no matter which are in their working or health status, we develop the first fixable **BODIPY** (boron-dipyrromethene) rotor, named **Vis-A**. **Vis-A** contains an aldehyde as anchor to react with aminos of proteins, which make it immobilizable in mitochondria. **Vis-B**, the reference compound without such anchor unit, is also synthesized. Both **Vis-A** and **Vis-B**, show excellent mitochondrial targetability, as good as the commercially available mitochondrial dye (Mito Tracker Deep Red). However, when cells are chemically treated to decrease the mitochondrial potential, only **Vis-A** continues emitting strong fluorescence in mitochondria, but the signals of **Vis-B** and Mito Tracker Deep Red completely disappear. This comparison confirms that **Vis-A** not only specifically localizes in mitochondria, but also can stably retain there. Then, **Vis-A** is applied to detect the mitochondrial viscosity of living cells by Fluorescence Lifetime Imaging (**FLIM**). Especially, with the aid of **Vis-A**, the changes of viscosity under typical pathological conditions (i.e., treatment with rotenone and carbonylcyanide-m-chlorophenylhydrazone, (**CCCP**) for mitochondria) are monitored by **FLIM**.

### Introduction

Mitochondria, known as power houses, play critical roles in cellular viability and the overall health. They are in charge of energy generation through the degrade of nutrients, which is the prerequisite for cells to maintain homeostasis and function properly.<sup>1</sup> Additionally, if mitochondrial microenvironment factors deviate from normal levels, mitochondria may go wrong to induce cells' malfunctions or even death.<sup>2-6</sup> Therefore, it is important to detect microenvironment changes in mitochondria.

After years of efforts from many research teams, quite a few chemical probes have been developed to sense and image environmental factors in the mitochondria, such as metal ion,<sup>7-14</sup> redox environment,<sup>15-29</sup> polarity,<sup>30-33</sup> viscosity,<sup>34-37</sup> pH,<sup>38-42</sup> and temperature.<sup>43</sup> Almost all these probes contain positively charged unit, which enables them to be accumulated in mitochondria, due to the attraction by the negative mitochondrial potential.<sup>44-48</sup> However, there still exists one big challenge. It is well known, under some pathological conditions, mitochondrial potential will be considerably decreased. Under these circumstances, probe molecules will

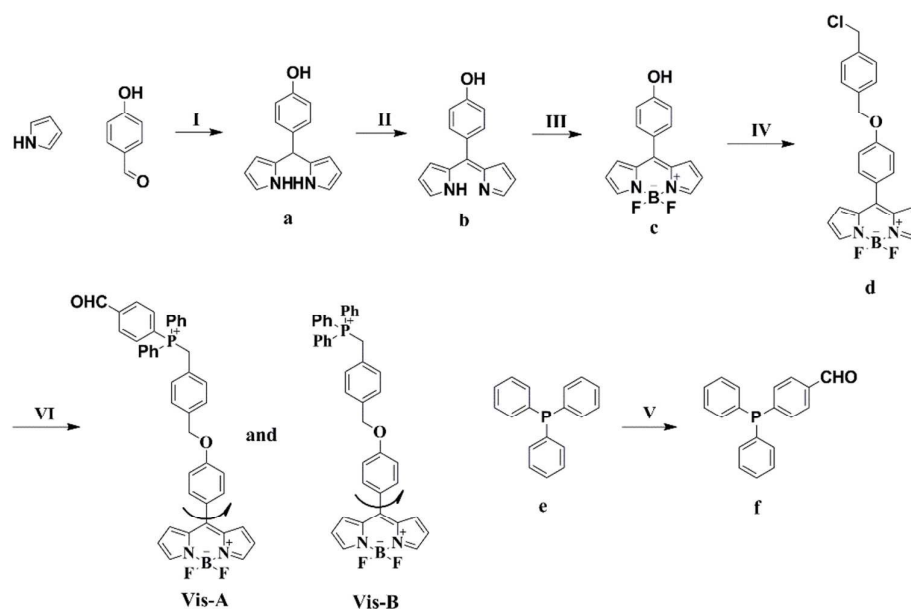
diffuse away from mitochondria for the lowering of the attraction. Thus, almost all those mitochondria targeted probes might be unsuitable for the studies on abnormal mitochondria, since they cannot stably retain there. In principle, this critical problem can be solved by fixation of probes in mitochondria by the formation of chemical bonds. But, to the best of our knowledge, only two cases on this topic have been reported recently. In 2014, Lee *et al* developed a fixable mitochondrial pH probe.<sup>38</sup> In 2015, our group reported a fixable polarity probe, which was used for quantitative detection of mitochondrial membrane potential in pathological conditions.<sup>30</sup>



Scheme 1. Working Principle of Mitochondrial Viscosity Probes.

<sup>a</sup> State Key Laboratory of Fine Chemicals, Dalian University of Technology, Dalian 116024, China, \*Email: xiaoyi@dlut.edu.cn.

† Footnotes relating to the title and/or authors should appear here. Electronic Supplementary Information (ESI) available: [details of any supplementary information available should be included here]. See DOI: 10.1039/x0xx00000x



**Scheme 2.** Synthetic routes for **Vis-A** and **Vis-B**. (I) 4-Hydroxybenzaldehyde/pyrrole/TFA, rt, 12 h, 94%; (II) DDQ, DCM, rt, 1 h, 90%; (III)  $\text{BF}_3 \cdot \text{Et}_2\text{O}$ /DIEA, PhMe, 70 °C, 0.5 h, 75%; (IV) 1,4-bis(chloromethyl)benzene/ $\text{K}_2\text{CO}_3$ , MeCN, reflux, 15 min, 90%; (V) 4-Bromobenzaldehyde/NaI/Pd/C, DMF, 160°C, 8 h, 35%; (VI) e or f/NaI, MeCN, reflux, 6 h, 95% or 45%.

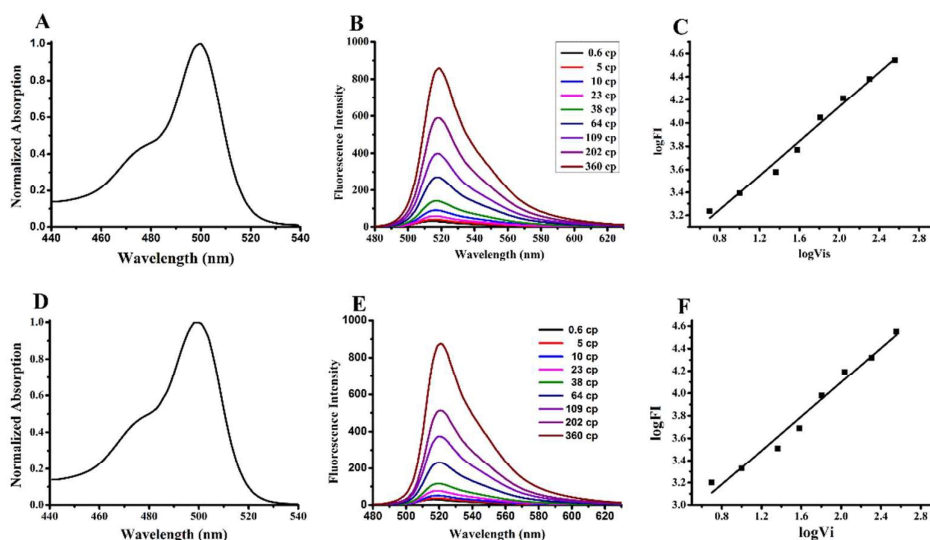


**Figure 1.** A: The absorption of **Vis-A** in methanol; B: Fluorescence spectra of **Vis-A** in methanol/glycerol mixtures; C: The relationship between fluorescence intensity and the viscosity; D: The absorption of **Vis-B** in methanol; E: Fluorescence spectra of **Vis-B** in methanol/glycerol mixtures; F: The relationship between fluorescence intensity and the viscosity.

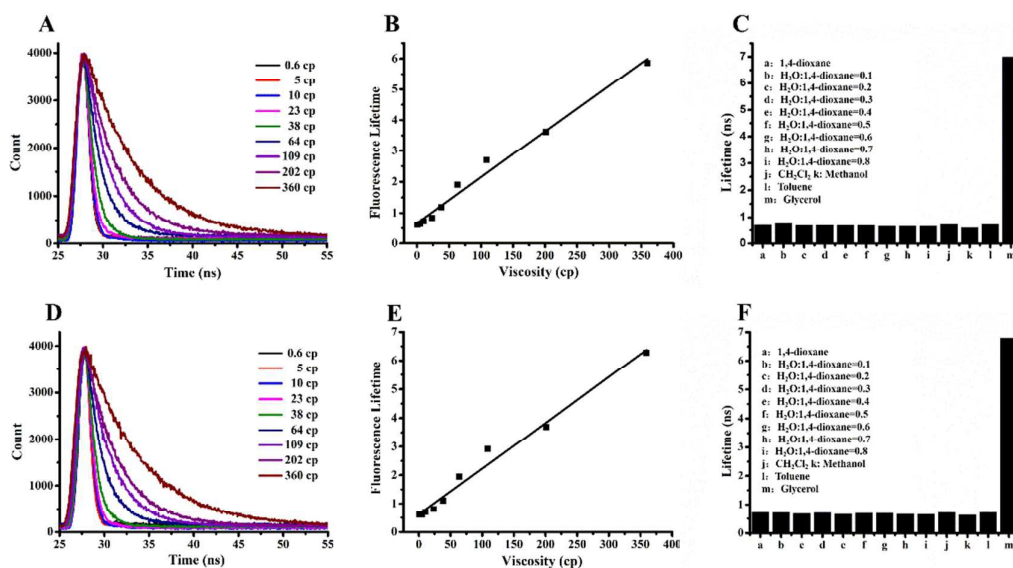


**Figure 2.** A: The fluorescence lifetime spectra at 520 nm for 3  $\mu\text{M}$  **Vis-A** in methanol/glycerol mixtures with varying proportions to adjust the viscosity; B: The relationship of **Vis-A** between the fluorescence intensity and the viscosity; C: The fluorescence lifetime of **Vis-A** responses to different polar solution. D: The fluorescence lifetime spectra at 520 nm for 3  $\mu\text{M}$  **Vis-B** in methanol/glycerol mixtures with varying proportions to adjust the viscosity; E: The relationship of **Vis-B** between the fluorescence intensity and the viscosity; F: The fluorescence lifetime of **Vis-B** responses to different polar solution.

In this work, we focus on probes for mitochondrial viscosity that is known to influence the signalling interaction of the biomolecules and chemicals. Abnormal viscosity variation in the mitochondrial matrix may induce changes in mitochondrial network organization, and further influence metabolite diffusion, which, consequently, are related to cellular aspects of many diseases and malfunctions, such as cell malignancy, atherosclerosis, diabetes, and Alzheimer's disease.<sup>49-51</sup> So far, there is not any report on a viscosity probe immobilized the mitochondria. Therefore, our aim is to design a practical probe for quantifying viscosity in all kinds of mitochondria, no matter their working or health status.

Based on the above consideration, we develop the first fixable probe for mitochondrial viscosity. As shown in Scheme 1, the key innovation of this viscosity probe, **Vis-A**, compared with several previously reported ones is its possession of a reactive aldehyde that can form stable covalent bond with aminos in proteins. In this paper, we confirm the applicability of **Vis-A**, in terms of its viscosity responsiveness, mitochondria-targeting specificity, and its stable retention in abnormal mitochondria. And we also apply **Vis-A** to monitor the viscosity changes under typical pathological conditions.

## Results and discussion

### Design and synthesis

There are several considerations in the molecular design of probe **Vis-A**. The cationic triphenylphosphonium is expected to facilitate the selective accumulation of the probe in mitochondria.<sup>44</sup> And the rotor unit provides sensitivity toward the viscosity, due to the free rotation around the single bond connecting the **BODIPY** core and the phenyl group.<sup>34, 52</sup> The fluorescence lifetime of the probe shows the linear relationship

with media viscosity, which provides the basis for monitoring mitochondrial viscosity *via* fluorescence lifetime imaging (FLIM). Last but not the least, probe **Vis-A** contains aldehyde, which can react with an amino of the proteins and be immobilized permanently on the proteins (**Scheme 1**). According to one of our recent studies, the first case of reactive aldehyde conjugated to a triphenylphosphonium moiety proved successful in targeting and fixing a probe onto the mitochondrial proteins.<sup>30</sup>

The probes, **Vis-A** and **Vis-B**, are synthesized very efficiently. The synthesis procedures are illustrated in **Scheme 2**. The reaction conditions and structural characterization are described in the Experimental section.

### Photophysical properties of **Vis-A** and **Vis-B**

To characterize the spectral properties of the sensors, we first study the absorption and the emission of the probes in methanol. Their maximum absorption of the wavelength is at 501 nm and their strongest fluorescence wavelength is at 517 nm in methanol. There is a very large change of the fluorescent intensity of the probes at various viscosities of the solvents (**Figure 1**). The probes show very weak fluorescent intensity in low-viscosity media and they show highly fluorescent intensity in viscous glycerol. These results are attributable to viscosity-dependent rotation of the C–C bond between the **BODIPY** and the phenyl unit, where the rotation through the C–C bond is restricted in the presence of a highly viscous solvent, such as glycerol, and the excited energy is reserved for emission without nonradioactive energy dissipation throughout the rotation. And the relationship between the fluorescence intensity and viscosity is showed in **figure 1C** and **1F**. The fluorescence intensity is influenced by concentration of the

probes and lasers. So we investigate the relationship between the fluorescence lifetime of the probes and the viscosity.

The fluorescence lifetimes of both the probes are measured in a series of viscosity gradient buffers, which are composed of methanol and glycerol in various proportions. Interestingly, the fluorescence lifetime of **Vis-A** at 520 nm increases gradually from 0.6ns to 5.9ns as the viscosity increases from 0.6cp to 360cp (**Figure 2A**). And the fluorescence lifetime of **Vis-B** at 520nm increases gradually from 0.6ns to 6.3ns as the viscosity increases from 0.6cp to 360cp (**Figure 2D**). In particular, there are good linear relationships observed between fluorescence lifetimes and solvent viscosity of the both probes ( $R^2 = 0.99$ ) (**Figure 2B**, and **2E**).

Selectivity is the most important requirement for all kinds of detection methods. For some viscosity probes, their fluorescence properties were found to be also highly sensitive to solvent polarity.<sup>53</sup> This will be problematic for the applications in the complex intracellular environment, because it will be hardly possible to distinguish the effect of viscosity to fluorescence from that of polarity. In order to confirm that the fluorescence lifetimes of our probes **Vis-A** and **Vis-B** are selectively responsive to viscosity changes but independent on polarity, we decide to carry out a measurement in several solvents with different polarity. According to a literature,<sup>54</sup> in the mixtures of water and 1,4-dioxane, a series of polarity gradient systems can be obtained by tuning the ratio of the two

solvent components. As shown in **figure 2C**, in all the water-dioxane mixed solvents, fluorescence lifetimes of **Vis-A** are very similar (around 0.68ns). We also measure fluorescence lifetime in low-polarity solvents *i.e.* toluene and dichloromethane, and the similar values are detected. These results indicate that fluorescence lifetime of **Vis-A** is insensitive to the variation of solvent polarity. Interestingly, when glycerol is used as solvent, the fluorescence lifetime value becomes very large (7.0ns). The longer lifetime in glycerol can be attributed to the high viscosity of this solvent and is not related to its polarity. The same conclusion for **Vis-B** can also be made, according to **figure 2F**. The excellent selectivity of **Vis-A** and **Vis-B** for viscosity is inherited to the parent BODIPY rotor. Therefore, our probes have great potential in viscosity detection in complex biological environments.

#### Localization stabilities of **Vis-A** and **Vis-B** in mitochondria

Colocalization studies of **Vis-A** and **Vis-B** with Mito Tracker Deep Red (Commercial mitochondrial tracker) have been conducted in 7721 cells, HeLa cells, and MCF-7 cells. As demonstrated in **figure 3**, **Vis-A** or **Vis-B** emits green fluorescence signals in channel 1, while the commercial mitochondrial tracker emits red signals in channel 2. The merged images (**Figure 3C** and **3G**) indicate that the two channel images overlap very well, confirming that the both probes can specially localize in the mitochondria of the living

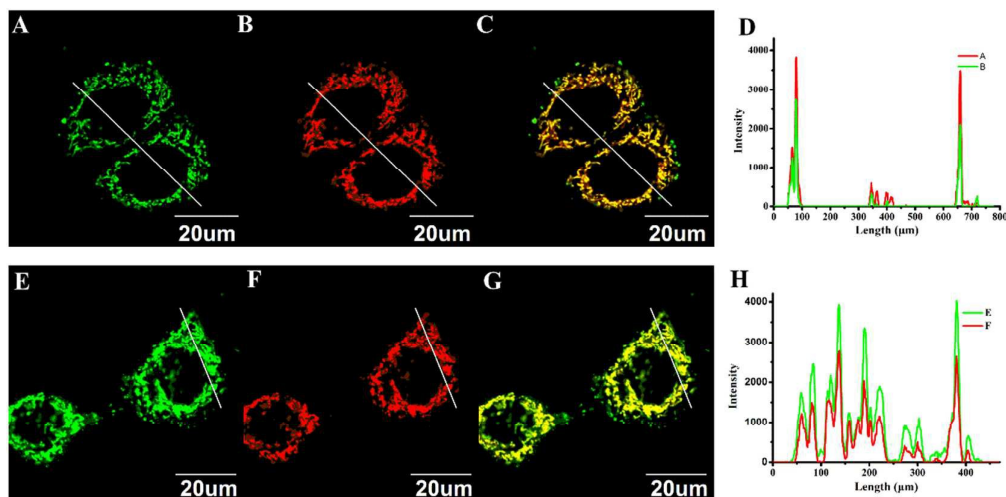


**Figure 3.** Colocalization imaging studies of **Vis-A** and **Vis-B** in 7721 cells. A **Vis-A** Channel 1:  $\lambda_{ex}=488\text{nm}$ ,  $\lambda_{em}=500\text{-}550\text{nm}$ . B Mito Tracker Deep Red Channel 2:  $\lambda_{ex}=635\text{nm}$ ,  $\lambda_{em}=655\text{-}755\text{nm}$ . C overlay of A and B (Pearson coefficient 0.97). E: **Vis-B** Channel 1:  $\lambda_{ex}=488\text{nm}$ ,  $\lambda_{em}=500\text{-}550\text{nm}$ . F Mito Tracker Deep Red Channel 2:  $\lambda_{ex}=635\text{nm}$ ,  $\lambda_{em}=655\text{-}755\text{nm}$ . G overlay of E and F (Pearson coefficient 0.92). D and H: Intensity profile of ROIs across the cells.

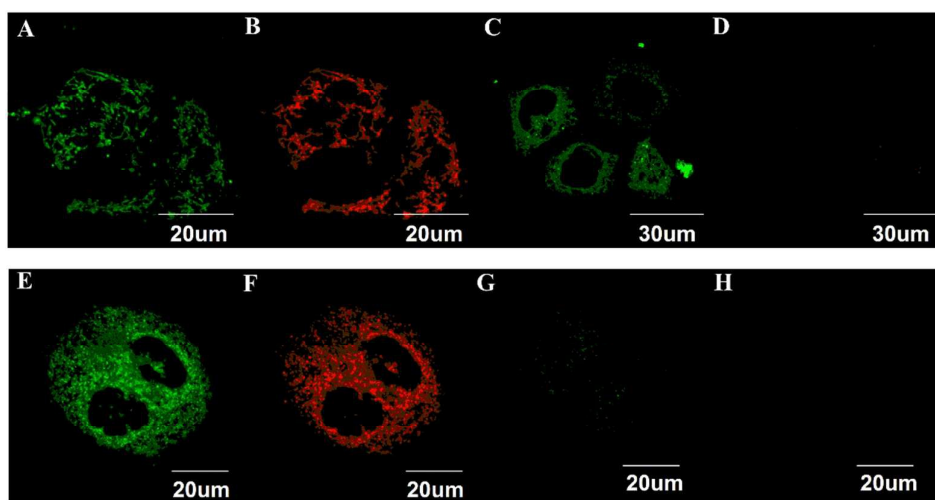


**Figure 4.** Imaging studies of **Vis-A** and **Vis-B** stain in 7721 cells. A, and B: The cells are treated with **Vis-A** (2  $\mu\text{M}$ ) and Mito Tracker Deep Red (0.5  $\mu\text{M}$ ) for 90 min, washed three times by PBS. C and D: The cells are treated with **Vis-A** (1  $\mu\text{M}$ ) and Mito Tracker Deep Red (0.5  $\mu\text{M}$ ) for 90 min, washed three times by PBS, cultured with four percent formaldehyde solution for 1 hours at 4  $^{\circ}\text{C}$ , and then washed by the solution (ethanol : PBS = 1 : 5) for three times. A and C **Vis-A** Channel 1:  $\lambda_{\text{ex}}=488\text{nm}$ ,  $\lambda_{\text{em}}=500\text{-}550\text{nm}$ . B and D Mito Tracker Deep Red Channel 2:  $\lambda_{\text{ex}}=635\text{nm}$ ,  $\lambda_{\text{em}}=655\text{-}755\text{nm}$ ; E and F: The cells are treated with **Vis-B** (1  $\mu\text{M}$ ) and Mito Tracker Deep Red (0.5  $\mu\text{M}$ ) for 90 min, washed three times by PBS. G and H: The cells are treated with **Vis-B** (1  $\mu\text{M}$ ) and Mito Tracker Deep Red (0.5  $\mu\text{M}$ ) for 90 min, washed three times by PBS, cultured with four percent formaldehyde solution for 1 hours at 4  $^{\circ}\text{C}$ , and then washed by the solution (ethanol : PBS = 1 : 5) for three times. E and G **Vis-B** Channel 1:  $\lambda_{\text{ex}}=488\text{nm}$ ,  $\lambda_{\text{em}}=500\text{-}550\text{nm}$ . F and H Mito Tracker Deep Red Channel 2:  $\lambda_{\text{ex}}=635\text{nm}$ ,  $\lambda_{\text{em}}=655\text{-}755\text{nm}$ .

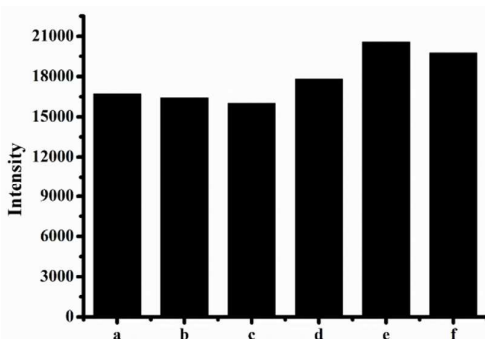


**Figure 5.** Flow cytometric analysis of MCF-7 cells. a, b, and c: The fluorescence intensity of the cells which are treated with **Vis-A** (4  $\mu\text{M}$ ) for 90 min, washed three times by PBS. d, e, and f: The fluorescence intensity of the cells which are treated with **Vis-A** (4  $\mu\text{M}$ ) for 90 min, washed three times by PBS, cultured with four percent formaldehyde solution for 1 hours at 4  $^{\circ}\text{C}$ , and then washed by PBS for three times.

cells. The changes in the intensity profile of linear regions of interest (ROIs) (Probes and commercial tracker) tend toward synchronization (Figure 3D and 3H). And the high Pearson's coefficients are obtained (**Vis-A**: Pearson coefficient 0.92 in 7721 cells; **Vis-B**: Pearson coefficient 0.97 in 7721 cells). The other images obtained in the colocalization studies are in the supporting information. Above investigation results confirm that both **Vis-A** and **Vis-B** target mitochondria specifically, because of the attraction from negative potentials in the mitochondria of the living cells.

As we have mentioned in the introduction section, an ideal mitochondrial probe should not only work in the normal mitochondria with relatively high potentials, but also it should continue working during the pathological processes in which the potential might be lowered considerably. To verify that **Vis-A** will permanently retain in mitochondria, we carry out another

set of colocalization imaging experiments under extreme conditions, as demonstrated in figure 4. 7721 cells are treated and cultured with four percent formaldehyde solution, which results in cell death and the complete elimination of mitochondrial potential.

As is expected, before and after the treatment, **Vis-A** exhibits strong intracellular fluorescence (Figure 4A and 4C), which means the decrease of mitochondrial potential will not drive **Vis-A** away from mitochondria. In contrast, the initially strong fluorescence signals of **Vis-B** and Mito Tracker Deep Red decrease remarkably (Figure 4G) or even disappear (Figure 4H) after the same treatment, indicating that they no longer stay in the mitochondria of the dead cells. And we also perform the same imaging experiments on other type of cells, e.g. MCF-7 and Hela cells (see supporting information) treated with formaldehyde. Again, the stable retention of **Vis-A** in mitochondria is observed. Since the only structural difference between **Vis-A** and **Vis-B** is the presence or absence of one aldehyde group, it is logical to ascribe the immobilization of **Vis-A** in mitochondria to this anchoring group.

In order to further prove the high efficiency of **Vis-A** to react with mitochondrial proteins, flow cytometry analysis is used to quantitatively evaluate fixation-induced changes of fluorescence intensity. We divide the flow cytometry experiments into two sets. First one is the control experiment without formaldehyde fixation, in which MCF-7 cells are incubated with **Vis-A** for 90 min and then washed three times by PBS. In second set, the cells are stained with the **Vis-A** for 90 min, washed three times by PBS, then treated with four percent formaldehyde solution for 1 hours at 4  $^{\circ}\text{C}$ , and finally washed by PBS three times. Then flow cytometry analyses are conducted for both groups of cells. The changes of intracellular fluorescence intensity are recorded in figure 5. Surprisingly, the fluorescence intensity of the formaldehyde-fixed cells is not

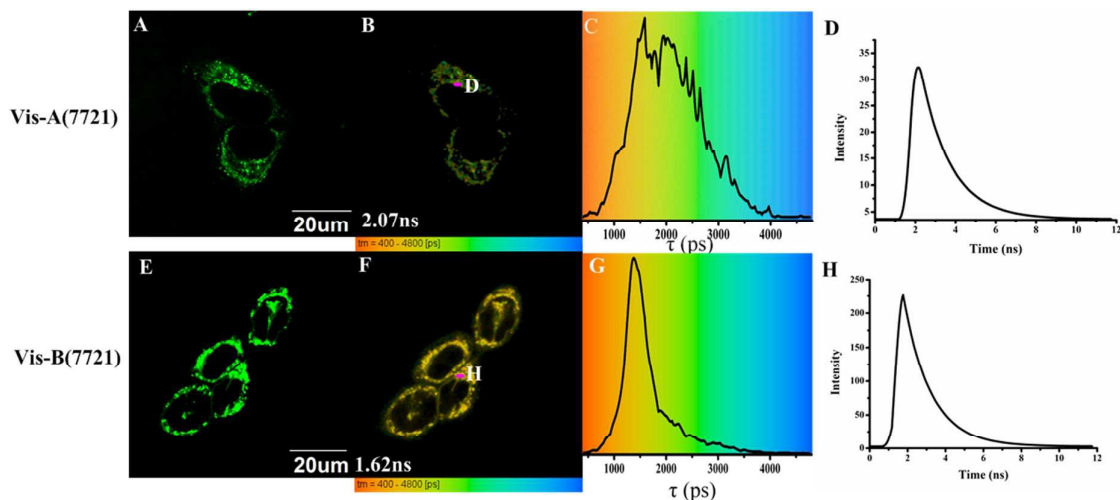


**Figure 6.** Imaging studies of **Vis-A** and **Vis-B** stain in 7721 cells. A: Fluorescence imaging of **Vis-A** in 7721 cells. B: Fluorescence life time imaging of **Vis-A** in 7721 cells. C: Fluorescence lifetime distribution histogram for B. D: The fluorescence decay curve of point D in image B. E: Fluorescence imaging of **Vis-B** in 7721 cells. F: Fluorescence lifetime imaging of **Vis-B** in 7721 cells. G: Fluorescence lifetime distribution histogram for E. H: The fluorescence decay curve of point H in image F. 7721 cells are treated with **Vis-A** (1  $\mu\text{M}$ ) for 90 min, washed three times by PBS. 7721 cells are treated with **Vis-B** (2  $\mu\text{M}$ ) for 90 min, washed three times by PBS.

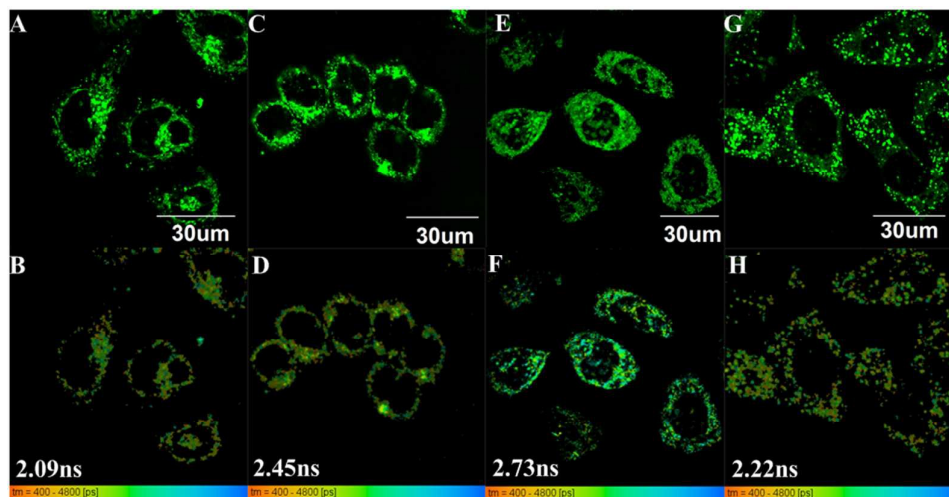


**Figure 7.** 7721 cells are treated with **Vis-A** (2  $\mu\text{M}$ ) for 90 min, washed three times by PBS. A, C, E, and G: Fluorescence imaging of **Vis-A** in 7721 cells. B(A), D(C), F(E), and H(G): Fluorescence life time imaging of **Vis-A** in 7721 cells. A and B: The control group. C and D: The cells are stimulated by rotenone (10  $\mu\text{M}$ ) for 8.5h. E and F: The cells are stimulated by rotenone (10  $\mu\text{M}$ ) for 18h. G and H: The cells are stimulated by **CCC1** (100  $\mu\text{M}$ ) for 3h.

lower but is even stronger than that of untreated cells. Our explanation is that, in the fixed cells, the local viscosity of mitochondria is much higher than that of the normal living cells. The fluorescence enhancement caused by higher viscosity is more pronounced than the possible fluorescence decrease resulted from the washed-out of the unfixed probes. Although above flow cytometry analysis fails in determining the probe-fixation percentage, it at least indirectly proves that the dye fixation efficiency is high sufficiently for further fluorescence imaging investigations.

#### Monitoring normal and abnormal mitochondrial viscosity

In combination **FLIM**, **Vis-A** and **Vis-B** are reliable tools for quantifying the local viscosity within mitochondria. **Figure 6** shows **FLIM** images of 7721 cells, in which fluorescence lifetime in the mitochondria has been mapped with considerable spatial resolution. In the **FLIM** image **6B**, the average fluorescence lifetime of **Vis-A** is 2.07ns, which is obtained from the fluorescence lifetime distribution histogram. Thus the average viscosity around **Vis-A** in mitochondria is determined to be about 95cp, according to our calibration graph in **figure 2B**. And the average fluorescence lifetime of **Vis-B** is 1.62ns (**Figure 6F** and **6G**), indicating the average viscosity around **Vis-B** is about 63cp. It is interesting that **Vis-A** and **Vis-B**

possessing the same rotor unit give different values of mitochondrial viscosity. We explain this difference by the different location: **Vis-A** is covalently bound to proteins, while the unbound **Vis-B** is located in the lipid bilayer of mitochondrial inner membranes. It is possible that macromolecular structures of proteins contribute to a larger viscosity reflected by the longer fluorescence lifetime of **Vis-A**.

Also noticeable is the wider fluorescence lifetime distribution histogram of **Vis-A** (**Figure 6C**) than that of **Vis-B** (**Figure 6G**). This might be due to the existence of many aminos in different sites of proteins with different structures, which produces quite different local viscosity around the bound **Vis-A** molecules. The above regulations obtained in 7721 cells are also observed when **Vis-A** and **Vis-B** are used to label other type of cells e.g. MCF-7 cells (supporting information).

The FLIM images (**Figure 6B** and **6F**) exhibit high spatial resolution almost as good as corresponding confocal images (**Figure 6A** and **6E**). The fluorescence lifetime distribution is so clearly mapped that it is feasible to determine the fluorescence lifetimes/viscosities of single mitochondria. For example, we randomly choose two regions (**D** and **H**) in cells, and obtained their fluorescence decay curves (**Figure 6D** and **6H**) that are as precise as those previously detected in solution (**Figure 2A** and **2D**).

As we mentioned, we hope to monitor the viscosity changes in the abnormal mitochondria. We have proved that, the immobilized **Vis-A** will permanently retain and continue emitting in mitochondria. Naturally, our next work is to confirm applicability of **Vis-A** in the pathological processes that mitochondria undergo damages. For this sake, rotenone, a chemical affecting cell respiration by inhibiting the transfer of electronic chain in mitochondria, is used to stimulate 7721 cells.<sup>55-59</sup> During a 8.5h period of stimulation using rotenone (10  $\mu$ M), according to the fluorescence lifetime distribution histogram, FLIM images reveal that the fluorescence lifetime in mitochondria of 7721 cells changes from 2.0ns to 2.45ns (**Figure 7B** and **7D**), which means that the average viscosity of mitochondria around the probe **Vis-A** increases considerably. And after the cells are incubated with rotenone for 18h, the average fluorescence lifetime further increases to 2.73ns (**Figure 7F**), indicating that further extension of treatment time will result in a slower increase in mitochondrial viscosity.

And the other stimulating agent is carbonylcyanide-m-chlorophenylhydrazone (**CCCP**), which is used to fast abolish the inner mitochondrial membrane potential, as this agent is one of the representative uncouplers for mitochondria-related pathology and pharmacology.<sup>60</sup> After the cells are stained with **CCCP** (100 $\mu$ M) for 3h, **FLIM** images indicate that the fluorescence lifetime in mitochondria of MCF-7 cells increases from 2.09ns to 2.22ns, which shows that the average viscosity of mitochondria around the probe **Vis-A** increases (**Figure 7H**). Although **CCCP** induced the fluorescence lifetime of the probes is not so pronounced as rotenone-induced, the former is faster. And it is also observed that **CCCP** stimulation causes a remarkable morphological change. As shown in **figure 7G** and **7H**, mitochondria turn from filamentary organizations to punctual structures, and it seems that the number of

mitochondria increase greatly. Thus, under the above pathological conditions, our probe **Vis-A** demonstrates the applicability to quantify the changes of mitochondrial viscosity and monitor mitochondrial morphology simultaneously.

## Conclusion

In conclusion, we have developed **Vis-A**, a new probe that can specifically target mitochondria and quantify local viscosity by its fluorescence lifetime. Compared with other viscosity probes, **Vis-A** contains a formyl group to react with aminos of proteins. For this reason, **Vis-A** can be permanently immobilized into mitochondria *via* forming covalent bond. This feature of **Vis-A** is helpful to overcome the non-fixed probes' problem of unstable mitochondrial localization. Such advantage of **Vis-A** is confirmed in the applications under two typical pathological conditions that damage mitochondria. Cells are stimulated with rotenone and **CCCP**. In both cases, apparent increases in mitochondrial viscosity are quantified by FLIM imaging with the aid of **Vis-A**. And it is believed that **Vis-A** provides a strategy in inspecting mitochondrial viscosity and in diagnosis of mitochondria related diseases.

## Experimental section

### Culture cells

MCF-7 cells, 7721 cells, and HeLa cells are obtained from Institute of Basic Medical Sciences (IBMS) of Chinese Academy of Medical Sciences (CAMS). All cell lines are maintained under standard culture conditions (atmosphere of 5% CO<sub>2</sub> and 95% air at 37 °C) in RPMI 1640 medium or DMEM medium, supplemented with 10% FBS (fetal bovine serum). The cells is used after the cells in the exponential phase of growth on 35 mm glass bottom culture dishes ( $\Phi$  20 mm) for 1 day.

### Synthesis

All chemicals are obtained from commercial suppliers and used without further purification. The 400 (<sup>1</sup>H) MHz NMR and 100 (<sup>13</sup>C) MHz NMR spectra are registered at room temperature on a 400 MHz spectrometer using perdeuterated solvents as internal standard. Images are acquired with a confocal microscopy from OLYMPUS.

General procedure for the synthesis of the probe and the probe's derivatives

**Preparation of a** 4-Hydroxybenzaldehyde (6 g, 49 mmol) is added to freshly distilled pyrrole under the protection of argon.<sup>61</sup> And then trifluoroacetic (0.2 ml) is dropped in the solution. The reaction mixture is stirred at room temperature for 12h. Excess of pyrrole is distilled under reduced pressure to give the black liquid, which is purified by silica gel flash chromatography using CH<sub>2</sub>Cl<sub>2</sub>/CH<sub>3</sub>OH (200:1 to 50:1) as eluent to afford compound a (11g, yields 94%). Compound a obtained as a grey solid is used for the next step without further purification.

**Preparation of b:** Compound a (1g, 4.2 mmol) is dissolved in CH<sub>2</sub>Cl<sub>2</sub> (20 mL) and then DDQ (1.1g 5.0mmol) is added to the

solution. The mixture is stirred for 1h. Filter out solid and then the solvent is removed under reduced pressure to give the crude black product, which is purified by silica gel flash chromatography using CH<sub>2</sub>Cl<sub>2</sub>/CH<sub>3</sub>OH (200:1 to 40:1) as eluent to afford compound b (0.9g, yields 90%). Compound b obtained as a grey solid is used for the next step without further purification.

**Preparation of c:** Compound b (4.23 mmol, 1 g) is added to a 15 mL toluene. The mixture is heated to 70 °C. N-Ethyl-diisopropylamine (21.6 mmol, 3.7mL) is dropped to the solution. After the solution is stirred for 30min, ethyl ether boron fluoride is dropped to the solution. And the reaction is stirred at 70 °C for 2h. Then the solvent is removed under reduced pressure to give the crude black product, which is purified by silica gel flash chromatography using CH<sub>2</sub>Cl<sub>2</sub>/CH<sub>3</sub>OH (200:1 to 80:1) as eluent to afford compound c (0.9g, yields 75%).

<sup>1</sup>H NMR (400 MHz, CDCl<sub>3</sub>) δ 6.55 (m, 2H), 6.97 (m, 4H), 7.45 (d, 2H), 7.90 (s, 2H).

**Preparation of d:** Compound c (150 mg, 0.53 mmol) and 1, 4-bis(chloromethyl)-benzene (186mg, 1.06 mmol) are dissolved in acetonitrile (5 mL). Potassium carbonate (146 mg, 1mmol) is added to the solution and the solution is refluxed for 40min. The solvent is removed under reduced pressure to give the crude product, which is purified by silica gel flash chromatography using CH<sub>2</sub>Cl<sub>2</sub>/hexane (1:1) as eluent to afford compound d (202mg, yields 90%). m/z (TOF MS EI+): Calcd [M+] for C<sub>23</sub>H<sub>18</sub>BClF<sub>2</sub>N<sub>2</sub>O 422.1169, found 422.1176.

<sup>1</sup>H NMR (500 MHz, CDCl<sub>3</sub>) δ 7.92 (s, 2H), 7.54 (d, J = 8.7 Hz, 2H), 7.49 – 7.43 (m, 4H), 7.11 (d, J = 8.6 Hz, 2H), 6.96 (d, J = 4.0 Hz, 2H), 6.54 (d, J = 3.0 Hz, 2H), 5.16 (s, 2H), 4.61 (s, 2H).

<sup>13</sup>C NMR (126 MHz, CDCl<sub>3</sub>) δ 161.13 (s), 147.27 (s), 143.51 (s), 137.61 (s), 136.56 (s), 134.86 (s), 132.43 (s), 131.35 (s), 128.98 (s), 127.80 (s), 126.71 (s), 118.30 (s), 114.91 (s), 69.85 (s), 45.80 (s).

**Preparation of f:** 4-Bromoacetophenone (1 g, 5.4 mmol), 5% (w/w) palladium (287.3mg, 0.27mmol), triphenylphosphine (3.537 g, 13.5 mmol) and NaI (1.62 g, 10.8 mmol) are added to anhydrous DMF under nitrogen protection. The mixture is stirred at 160 °C for 8 h. The reaction mixture is cooled to room temperature. And the reaction mixture is filtrated to remove insoluble impurities, then the DMF is removed under reduced pressure. The residue is purified by silica gel column chromatography using eluent hexanes/CH<sub>2</sub>Cl<sub>2</sub> (3/1, v/v). A white solid is obtained (620 mg, 39.6 %).

**Preparation of Vis-A:** Compound d (23 mg, 0.054 mmol), NaI (70 mg, 0.54 mmol) and f (42 mg, 0.16 mmol) are dissolved in 3mL acetonitrile under nitrogen protection. The mixture is refluxed for 60min. Then the acetonitrile is removed under reduced pressure. The mixture is purified by column chromatography (gradient:CH<sub>2</sub>Cl<sub>2</sub>/CH<sub>3</sub>OH 40:1 → 15:1) to obtain Vis-A (34 mg, 80%). m/z (FTMS+p ESI): Calcd [M+] for C<sub>42</sub>H<sub>33</sub>BF<sub>2</sub>N<sub>2</sub>O<sub>2</sub>P<sup>+</sup>, 677.2335, found 677.2345.

<sup>1</sup>H NMR (500 MHz, CDCl<sub>3</sub>) δ 10.09 (s, 1H), 8.07 (dd, J = 11.9, 8.3 Hz, 2H), 8.02 (dd, J = 8.2, 3.1 Hz, 2H), 7.91 (s, 2H), 7.78 (dd, J = 13.0, 7.7 Hz, 6H), 7.61 (td, J = 7.9, 3.5 Hz, 4H),

7.53 (d, J = 8.7 Hz, 2H), 7.29 (dd, J = 8.2, 2.1 Hz, 2H), 7.25 (d, J = 8.1 Hz, 2H), 7.08 (d, J = 8.7 Hz, 2H), 6.95 (d, J = 4.0 Hz, 2H), 6.54 (d, J = 2.5 Hz, 2H), 5.09 (s, 2H).

<sup>13</sup>C NMR (126 MHz, CDCl<sub>3</sub>) δ 190.78 (s), 160.95 (s), 147.14 (s), 143.58 (s), 140.21 (d, J = 2.7 Hz), 136.95 (d, J = 4.2 Hz), 135.42 (dd, J = 10.0, 6.6 Hz), 134.84 (s), 134.63 (d, J = 9.9 Hz), 132.45 (s), 132.09 (d, J = 5.5 Hz), 131.36 (s), 130.34 (d, J = 12.7 Hz), 127.81 (d, J = 3.3 Hz), 126.81 (s), 124.56 (s), 123.89 (s), 118.37 (s), 117.24 (s), 116.56 (s), 114.93 (s), 69.60 (s), 30.38 (s).

**Preparation of Vis-B:** Compound d (23 mg, 0.054 mmol), NaI (70 mg, 0.54 mmol) and triphenylphosphine (40 mg, 0.16 mmol) are dissolved in 3mL acetonitrile under nitrogen protection. The mixture is refluxed for 40min. Then the acetonitrile is removed under reduced pressure. The mixture is purified by column chromatography (gradient:CH<sub>2</sub>Cl<sub>2</sub>/CH<sub>3</sub>OH 40:1 → 15:1) to obtain Vis-B (34 mg, 80%). m/z (FTMS+p ESI): Calcd [M+] for C<sub>41</sub>H<sub>33</sub>BF<sub>2</sub>N<sub>2</sub>OP<sup>+</sup>, 649.2386, found 649.2382.

<sup>1</sup>H NMR (500 MHz, CDCl<sub>3</sub>) δ 7.90 (s, 2H), 7.75 (ddd, J = 19.9, 10.3, 6.9 Hz, 9H), 7.63 (td, J = 7.9, 3.5 Hz, 6H), 7.51 (d, J = 8.7 Hz, 2H), 7.25 (d, J = 8.0 Hz, 2H), 7.19 (dd, J = 8.2, 2.3 Hz, 2H), 7.06 (d, J = 8.7 Hz, 2H), 6.95 (d, J = 4.0 Hz, 2H), 6.54 (dd, J = 4.1, 1.7 Hz, 2H), 5.32 (d, J = 14.4 Hz, 2H), 5.10 (d, J = 1.5 Hz, 2H).

<sup>13</sup>C NMR (126 MHz, CDCl<sub>3</sub>) δ 160.95 (s), 147.18 (s), 143.48 (s), 136.82 (d, J = 4.0 Hz), 135.14 (d, J = 2.9 Hz), 134.80 (s), 134.44 (d, J = 9.8 Hz), 132.41 (s), 131.89 (d, J = 5.5 Hz), 131.37 (s), 130.23 (d, J = 12.6 Hz), 127.72 (d, J = 3.3 Hz), 126.69 (s), 118.36 (s), 117.90 (s), 117.22 (s), 114.98 (s), 69.60 (s), 29.67 (s).

## Acknowledgements

This work was supported by the National Natural Science Foundation of China (nos. 21174022, 21376038, 21421005, and 21576040), the National Basic Research Program of China (no. 2013CB733702).

## Notes and references

1. Y.-L. P. Ow, D. R. Green, Z. Hao and T. W. Mak, *Nat. Rev. Mol. Cell Biol.*, 2008, **9**, 532-542.
2. D. C. Wallace, *Nat. Rev. Cancer*, 2012, **12**, 685-698.
3. P. M. Quiros, T. Langer and C. Lopez-Otin, *Nat. Rev. Mol. Cell Biol.*, 2015, **16**, 345-359.
4. L. Galluzzi, O. Kepp and G. Kroemer, *Nat. Rev. Mol. Cell Biol.*, 2012, **13**, 780-788.
5. B. C. Dickinson and C. J. Chang, *Nat. Chem. Biol.*, 2011, **7**, 504-511.
6. G. Masanta, C. H. Heo, C. S. Lim, S. K. Bae, B. R. Cho and H. M. Kim, *Chem. Commun.*, 2012, **48**, 3518-3520.
7. S. L. Sensi, D. Ton-That, J. H. Weiss, A. Rothe and K. R. Gee, *Cell Calcium*, 2003, **34**, 281-284.
8. K. Sreenath, J. R. Allen, M. W. Davidson and L. Zhu, *Chem. Commun.*, 2011, **47**, 11730-11732.

9. L. Xue, G. Li, C. Yu and H. Jiang, *Chem. Eur. J.*, 2012, **18**, 1050-1054.
10. G. Masanta, C. S. Lim, H. J. Kim, J. H. Han, H. M. Kim and B. R. Cho, *J. Am. Chem. Soc.*, 2011, **133**, 5698-5700.
11. E. M. Nolan, J. W. Ryu, J. Jaworski, R. P. Feazell, M. Sheng and S. J. Lippard, *J. Am. Chem. Soc.*, 2006, **128**, 15517-15528.
12. S. C. Dodani, S. C. Leary, P. A. Cobine, D. R. Winge and C. J. Chang, *J. Am. Chem. Soc.*, 2011, **133**, 8606-8616.
13. M. Taki, K. Akaoka, K. Mitsui and Y. Yamamoto, *Org. Biomol. Chem.*, 2014, **12**, 4999-5005.
14. H. Komatsu, N. Iwasawa, D. Citterio, Y. Suzuki, T. Kubota, K. Tokuno, Y. Kitamura, K. Oka and K. Suzuki, *J. Am. Chem. Soc.*, 2004, **126**, 16353-16360.
15. Y. Koide, Y. Urano, S. Kenmoku, H. Kojima and T. Nagano, *J. Am. Chem. Soc.*, 2007, **129**, 10324-10325.
16. F. Yu, P. Li, B. Wang and K. Han, *J. Am. Chem. Soc.*, 2013, **135**, 7674-7680.
17. H. Zhang, J. Liu, Y.-Q. Sun, Y. Huo, Y. Li, W. Liu, X. Wu, N. Zhu, Y. Shi and W. Guo, *Chem. Commun.*, 2015, **51**, 2721-2724.
18. F. Liu, T. Wu, J. Cao, H. Zhang, M. Hu, S. Sun, F. Song, J. Fan, J. Wang and X. Peng, *Analyst*, 2013, **138**, 775-778.
19. K. Xu, S. Sun, J. Li, L. Li, M. Qiang and B. Tang, *Chem. Commun.*, 2012, **48**, 684-686.
20. Y.-Q. Sun, J. Liu, H. Zhang, Y. Huo, X. Lv, Y. Shi and W. Guo, *J. Am. Chem. Soc.*, 2014, **136**, 12520-12523.
21. H. Yu, X. Zhang, Y. Xiao, W. Zou, L. Wang and L. Jin, *Anal. Chem.*, 2013, **85**, 7076-7084.
22. X. Wang, J. Sun, W. Zhang, X. Ma, J. Lv and B. Tang, *Chem. Sci.*, 2013, **4**, 2551-2556.
23. F. Meng, Y. Liu, X. Yu and W. Lin, *New J. Chem.*, 2016, **40**, 7399-7406.
24. Y. Chen, C. Zhu, Z. Yang, J. Chen, Y. He, Y. Jiao, W. He, L. Qiu, J. Cen and Z. Guo, *Angew. Chem. Int. Ed.*, 2013, **52**, 1688-1691.
25. H.-W. Liu, S. Xu, P. Wang, X. Hu, J. Zhang, L. Yuan, X. Zhang and W. Tan, *Chem. Commun.*, 2016, **52**, 12330-12333.
26. X. Yang, Y. Zhou, X. Zhang, S. Yang, Y. Chen, J. Guo, X. Li, Z. Qing and R. Yang, *Chem. Commun.*, 2016, **52**, 10289-10292.
27. X. Wu, A. Shao, S. Zhu, Z. Guo and W. Zhu, *Sci. China. Chem.*, 2016, **59**, 62-69.
28. H. Yu, Y. Xiao and L. Jin, *J. Am. Chem. Soc.*, 2012, **134**, 17486-17489.
29. X. Zhang, B. Wang, C. Wang, L. Chen and Y. Xiao, *Anal. Chem.*, 2015, **87**, 8292-8300.
30. B. Wang, X. Zhang, C. Wang, L. Chen, Y. Xiao and Y. Pang, *Analyst*, 2015, **140**, 5488-5494.
31. H. Yuan, H. Cho, H. H. Chen, M. Panagia, D. E. Sosnovik and L. Josephson, *Chem. Commun.*, 2013, **49**, 10361-10363.
32. N. Jiang, J. Fan, T. Liu, J. Cao, B. Qiao, J. Wang, P. Gao and X. Peng, *Chem. Commun.*, 2013, **49**, 10620-10622.
33. Z. Xu and L. Xu, *Chem. Commun.*, 2016, **52**, 1094-1119.
34. Z. Yang, Y. He, J.-H. Lee, N. Park, M. Suh, W.-S. Chae, J. Cao, X. Peng, H. Jung, C. Kang and J. S. Kim, *J. Am. Chem. Soc.*, 2013, **135**, 9181-9185.
35. M. Zhao, Y. Zhu, J. Su, Q. Geng, X. Tian, J. Zhang, H. Zhou, S. Zhang, J. Wu and Y. Tian, *J. Mater. Chem. B*, 2016, **4**, 5907-5912.
36. N. Jiang, J. Fan, S. Zhang, T. Wu, J. Wang, P. Gao, J. Qu, F. Zhou and X. Peng, *Sensors Actuators B: Chem.*, 2014, **190**, 685-693.
37. D. Su, C. Teoh, N. Gao, Q.-H. Xu and Y.-T. Chang, *Sensors*, 2016, **16**, 1397.
38. M. H. Lee, N. Park, C. Yi, J. H. Han, J. H. Hong, K. P. Kim, D. H. Kang, J. L. Sessler, C. Kang and J. S. Kim, *J. Am. Chem. Soc.*, 2014, **136**, 14136-14142.
39. A. R. Sarkar, C. H. Heo, L. Xu, H. W. Lee, H. Y. Si, J. W. Byun and H. M. Kim, *Chem. Sci.*, 2016, **7**, 766-773.
40. Y. Chen, C. Zhu, J. Cen, Y. Bai, W. He and Z. Guo, *Chem. Sci.*, 2015, **6**, 3187-3194.
41. M.-Y. Wu, K. Li, Y.-H. Liu, K.-K. Yu, Y.-M. Xie, X.-D. Zhou and X.-Q. Yu, *Biomaterials*, 2015, **53**, 669-678.
42. P. Li, H. Xiao, Y. Cheng, W. Zhang, F. Huang, W. Zhang, H. Wang and B. Tang, *Chem. Commun.*, 2014, **50**, 7184-7187.
43. M. Homma, Y. Takeji, A. Murata, T. Inoue and S. Takeoka, *Chem. Commun.*, 2015, **51**, 6194-6197.
44. R. A. J. Smith, C. M. Porteous, A. M. Gane and M. P. Murphy, *Proc. Natl. Acad. Sci. U. S. A.*, 2003, **100**, 5407-5412.
45. M. P. Murphy, *Trends Biotechnol.*, 1997, **15**, 326-330.
46. E. A. Liberman, V. P. Topaly, L. M. Tsofina, A. A. Jasaitis and V. P. Skulachev, *Nature*, 1969, **222**, 1076-1078.
47. J. Jose, A. Loudet, Y. Ueno, R. Barhoumi, R. C. Burghardt and K. Burgess, *Org. Biomol. Chem.*, 2010, **8**, 2052-2059.
48. B. C. Dickinson, D. Srikun and C. J. Chang, *Curr. Opin. Chem. Biol.*, 2010, **14**, 50-56.
49. G. Deliconstantinos, V. Villiotou and J. C. Stavrides, *Biochem. Pharmacol.*, 1995, **49**, 1589-1600.
50. O. Nativ, M. Shinitzky, H. Manu, D. Hecht, C. T. Roberts, D. LeRoith and Y. Zick, *Biochem. J*, 1994, **298**, 443-450.
51. S. G. Zubenko, U. Kopp, T. Seto and L. L. Firestone, *Psychopharmacology (Berl.)*, 1999, **145**, 175-180.
52. L. Wang, Y. Xiao, W. Tian and L. Deng, *J. Am. Chem. Soc.*, 2013, **135**, 2903-2906.
53. F. Zhou, J. Shao, Y. Yang, J. Zhao, H. Guo, X. Li, S. Ji and Z. Zhang, *Eur. J. Org. Chem.*, 2011, 4773-4787.
54. N. Jiang, J. Fan, F. Xu, X. Peng, H. Mu, J. Wang and X. Xiong, *Angew. Chem. Int. Ed.*, 2015, **54**, 2510-2514.
55. F. Dagani, F. Feletti and L. Canevari, *J. Neurochem.*, 1989, **53**, 1379-1389.
56. I. K. Srivastava, H. Rottenberg and A. B. Vaidya, *J. Biol. Chem.*, 1997, **272**, 3961-3966.
57. E. Pavlov, R. Aschar-Sobbi, M. Campanella, R. J. Turner, M. R. Gómez-García and A. Y. Abramov, *J. Biol. Chem.*, 2010, **285**, 9420-9428.
58. N. Baudry, E. Laemmel and E. Vicaut, *American Journal of Physiology - Heart and Circulatory Physiology*, 2008, **294**, H821-H828.
59. A. M. Beyer, M. J. Durand, J. Hockenberry, T. C. Gamblin, S. A. Phillips and D. D. Gutterman, *American Journal of Physiology - Heart and Circulatory Physiology*, 2014, **307**, H1587-H1593.
60. M. L. R. Lim, T. Minamikawa and P. Nagley, *FEBS Lett.*, 2001, **503**, 69-74.
61. A. N. Kursunlu, E. Guler, H. I. Ucan and R. W. Boyle, *Dyes and Pigments*, 2012, **94**, 496-502.

Fixable probe, named Vis-A, quantify mitochondrial viscosity of living cells by fluorescence lifetime imaging

